A Gravity-Compensation Algorithm for the Haptic Device Based on the Principle of Virtual Work and BP Neural Network

Shuo Wang, Zhiyuan Yan, Zhengxin Yang and Zhijiang Du*
State Key Laboratory of Robotics and System, Harbin Institute of Technology, Xidazhi Street, Harbin, China
**hitwangshuo@foxmail.com*

Keywords: Haptic device, Gravity-compensation, Principle of virtual work, BP neural network.

Abstract: The haptic device is the key facility in the master-slave minimally invasive surgery system, a gravity-compensation algorithm is proposed for this device. The structure of this device mentioned in this paper is a combination of serial and parallel structure, and it has 6 degrees of freedom. 3 motors are installed at 3 active joints respectively. In order to establish the dynamic equation of the haptic device, the device is simplified and the torque which is used to compensate the gravity is calculated by the principle of virtual work (Codourey A, 1998). Then the whole process of gravity-compensation is simulated under the environment of a dynamic software. After the comparison between the theoretical model and the simulation result, errors are shown and compensated through BP neural network, the performance of the gravity-compensation is improved.

1 INTRODUCTION

The master-slave minimally invasive surgery system has been widely used, it has numbers of advantages and they are recognized by the public (Okamura A M, 2011). The haptic device is very important in the whole system for the surgeon relies on it to feel the feedback force. The haptic device should not only meets the needs of high stiffness, low damping and small inertia, but also be able to compensate its own gravity (Wang and Gosselin, 1998). The methods which can realize gravity-compensation can be classified as mechanical method and dynamic method. Mechanical methods mainly include counterweight method, equivalent mass method and spring compensation method (Zhang L N, 2013); dynamic methods mainly contain Newton-Euler method, virtual work method and Lagrange method (You W, 2008).

In order to simplify the modelling process, the principle of virtual work is used to establish the dynamic model, it provides a theoretical basis for gravity-compensation. Then the haptic device is simulated by relative software and the simulation torque is obtained. After comparing the theoretical torque and simulation torque, errors are found. Then BP neural network is used to compensate the errors (Wu B, 2016).

2 HAPTIC DEVICE

The haptic device is made by the serial part and parallel part, as shown in Figure 1. It has 6 degrees of freedom, the parallel part has 3 degrees of freedom which are used to control the position of the slave device, the 3 degrees of freedom in the serial part controls the posture of the slave device. The gravity-compensation mentioned in this paper is carried out by the parallel part, and the gravity-compensation of the serial part is not discussed.

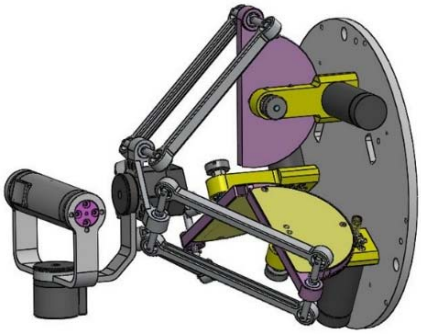

Figure 1: The haptic device.

The parallel part consists of 3 parts, namely moving platform, static platform and 3 identical branches, they are shown in Figure 2. Each branch has

Wang, S., Yan, Z., Yang, Z. and Du, Z.
A Gravity-Compensation Algorithm for the Haptic Device Based on the Principle of Virtual Work and BP Neural Network.
In *3rd International Conference on Electromechanical Control Technology and Transportation (ICECTT 2018)*, pages 599-605
ISBN: 978-989-758-312-4

7 revolute pairs, the semi-disc works as the active link, its joint works as the active joint, while the parallelogram mechanism works as the passive link.

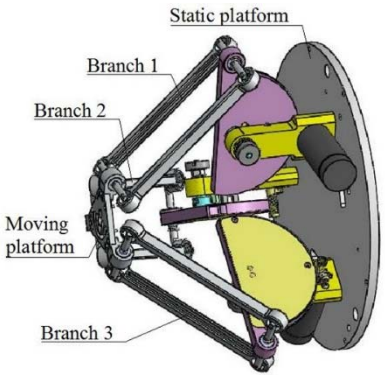

Figure 2: The parallel part.

3 GRAVITY-COMPENSATION

3.1 Simplification of mechanical model

Branches of the haptic device are made of hard aluminum alloy which has low density and mass, so their moment of inertia can be ignored. The mass of each branch can be divided into two equal parts, one is added to the joint of semi-disc, the other one is added to the joint of the static platform. When we analyse the parallel part we can simplify the serial part as a whole and add its mass to the moving platform. After simplification we name the new moving platform as synthetic moving platform and the new semi-disc as synthetic semi-disc mechanism. The simplified model is shown in Figure 3.

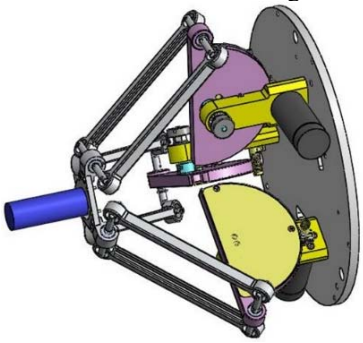

Figure 3: The simplified model.

3.2 Establishment of mechanical model

This haptic device has 3 active motors, if we only take gravity into consideration then the dynamic model can be described as:

$$\Gamma = M(\alpha)\ddot{\alpha} + C(\alpha,\dot{\alpha}) + G(\alpha) \quad (1)$$

In the equation, Γ is the 3×1 order joint moment vector, M is 3×3 order inertia matrix, C is centrifugal force and coriolis force, G is the 3×1 order gravity, α is the turning angle of the active joints.

If there is external force in the system the principle of virtual work can be described as:

$$\delta W = \sum_{j=1}^{N}[(F_j - m_j a_j)\cdot\delta r_j + (\tau_j - I\ddot{\alpha})\cdot\delta\alpha] = 0 \quad (2)$$

In the equation, δW is the sum of virtual work, F_j is external force, m_j is the particle mass, a_j is the particle acceleration, δr_j is the virtual displacement, τ_j is the external torque, I is moment of inertia, $\ddot{\alpha}$ is the angle acceleration and $\delta\alpha$ is virtual angle.

3.3 Establishment of dynamic equation

3.3.1 Analysis of the simplified model

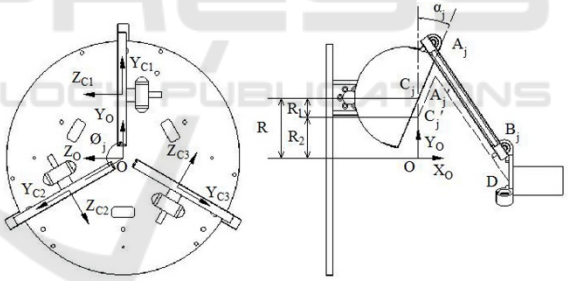

Figure 4: The coordinate system of the simplified model.

In Figure 4, the direction of $\{C_j' X_{Cj'} Y_{Cj'} Z_{Cj'}\}$ and $\{C_j X_{C_j} Y_{C_j} Z_{C_j}\}$ relative to $\{OX_O Y_O Z_O\}$ can be described with ${}^{O}T_{Cj}$. The angle between branch j and Y_O in plane $Y_O O Z_O$ is $\Phi_j = 2\pi(j-1)/3$ and $j = 1,2,3$, C_j is at the rotation center of the semi-disc. α_j is the turning angle of semi-disc and the clockwise direction is positive. $D = \begin{bmatrix} D_x & D_y & D_z \end{bmatrix}^T$ and it is the position of the moving platform. The branch length is a constant and if $k_j = \overrightarrow{A_j' D}$, then we have:

$$k_j = \overrightarrow{A_j D} = \overrightarrow{OD} - {}^{O}T_{Cj}(\overrightarrow{OC_j} + \overrightarrow{C_j A_j}) \quad (3)$$
$$= \begin{bmatrix} D_x \\ D_y \\ D_z \end{bmatrix} - {}^{O}T_{Cj}\left(\begin{bmatrix} 0 \\ R_2 \\ 0 \end{bmatrix} + \begin{bmatrix} L_1 \sin\alpha_j \\ L_1 \cos\alpha_j \\ 0 \end{bmatrix}\right)$$

$$\dot{k}_j = \begin{bmatrix} \dot{D}_x \\ \dot{D}_y \\ \dot{D}_z \end{bmatrix} + {}^{O}T_{Cj}\left(\begin{bmatrix} -L_1 \cos\alpha_j \\ L_1 \sin\alpha_j \\ 0 \end{bmatrix}\right)\dot{\alpha}_j = \dot{D} + e_j\dot{\alpha}_j \quad (4)$$

$$\dot{k}_j \cdot k_j{}^T + k_j \cdot \dot{k}_j{}^T = 0 \quad (5)$$

With equation (4) and (5) we have:

$$k_j{}^T \dot{D} + k_j{}^T e_j \dot{\alpha}_j = 0 \quad (6)$$

In the equations above we know that $j = 1,2,3$, then we simplify equation (6) based on $\dot{D} = J\dot{\alpha}$:

$$J = -\begin{bmatrix} k_1{}^T \\ k_2{}^T \\ k_3{}^T \end{bmatrix}^{-1}\begin{bmatrix} k_1{}^T e_1 & 0 & 0 \\ 0 & k_2{}^T e_2 & 0 \\ 0 & 0 & k_3{}^T e_3 \end{bmatrix} \quad (7)$$

After simplifying the derivative of equation (6):

$$\ddot{D} = -\begin{bmatrix} k_1{}^T \\ k_2{}^T \\ k_3{}^T \end{bmatrix}^{-1}\left(\begin{bmatrix} \dot{k}_1{}^T \\ \dot{k}_2{}^T \\ \dot{k}_3{}^T \end{bmatrix} J + Q\right)\dot{\alpha} + J\ddot{\alpha} \quad (8)$$

$$Q = \begin{bmatrix} \dot{k}_1{}^T e_1 + k_1{}^T \dot{e}_1 & 0 & 0 \\ 0 & \dot{k}_2{}^T e_2 + k_2{}^T \dot{e}_2 & 0 \\ 0 & 0 & \dot{k}_3{}^T e_3 + k_3{}^T \dot{e}_3 \end{bmatrix} \quad (9)$$

Based on $\ddot{D} = \dot{J}\dot{\alpha} + J\ddot{\alpha}$ and equation (8):

$$\dot{J} = -\begin{bmatrix} k_1{}^T \\ k_2{}^T \\ k_3{}^T \end{bmatrix}^{-1}\left(\begin{bmatrix} \dot{k}_1{}^T \\ \dot{k}_2{}^T \\ \dot{k}_3{}^T \end{bmatrix} J + Q\right) \quad (10)$$

After simplification, the mass of the synthesized moving platform can be described as:

$$m_s = m_c + m_d + \frac{3}{2}m_l \quad (11)$$

In this equation, m_s is the mass of the synthesized moving platform, m_c is the mass of the serial part, m_d is the mass of the original moving platform, m_l is the mass of a branch.

After simplification, the mass of the synthesized semi-disc can be described as:

$$m_b = m_h + \frac{1}{2}m_l \quad (12)$$

In this equation, m_b is the mass of the synthesized semi-disc, m_h is the mass of the original semi-disc.

The vector of synthesized semi-disc‘s center of mass can be described as:

$$\overrightarrow{R_{cm}} = \frac{m_h \vec{r}_h + \frac{1}{2}m_l \vec{r}_l}{m_h + \frac{1}{2}m_l} \quad (13)$$

In this equation, $\vec{r}_h$ is the vector of the semi-disc‘s center of mass relative to the semi-disc‘s rotation center, $\vec{r}_l$ is the vector of the centralized mass of the branch relative to the semi-disc‘s rotation center. With Figure 5 they can also be described as:

$$\vec{r}_h = \begin{bmatrix} -h\cos\alpha_j & h\sin\alpha_j & 0 \end{bmatrix}^T \quad (14)$$

$$\vec{r}_l = \begin{bmatrix} l\sin\alpha_j & l\cos\alpha_j & 0 \end{bmatrix}^T \quad (15)$$

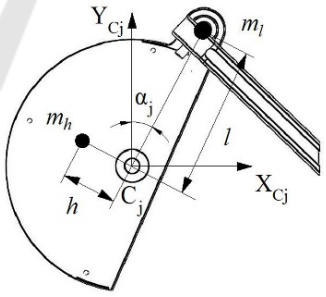

Figure 5: Semi-disc and its branch.

The gravity torque of the synthesized semi-disc can be described as:

$$\tau_{cm} = \left| {}^{O}T_{Cj}\overrightarrow{R_{cm}} \times (m_h + \frac{1}{2}m_l)\vec{g} \right| \quad (16)$$

In this equation $\vec{g} = \begin{bmatrix} 0 & -g & 0 \end{bmatrix}^T$.

The rotary inertia of the synthesized semi-disc can be described as:

$$I_b = I_h + I_l = I_o + m_h h^2 + \frac{1}{2} m_l L_1^2 \quad (17)$$

In this equation, I_h is the rotary inertia of the original semi-disc, I_l is the rotary inertia of the centralized mass of the branch, I_o is the rotary inertia of the original semi-disc relative to the semi-disc's mass of center.

3.3.2 Derivation of dynamic equation

During operation, the synthesized moving platform is mainly affected by gravity F_g and inertia force F_a. Based on the principle of virtual work we have:

$$(\Gamma + \Gamma_g + \Gamma_{cm})\delta\alpha = (I_b\ddot{\alpha} + \Gamma_a)\delta\alpha \quad (18)$$

$$\Gamma_g = J^T F_g = J^T m_s \vec{g} \quad (19)$$

$$\Gamma_a = J^T F_a = J^T m_s \ddot{D} \quad (20)$$

Equation (18) can also be described as:

$$\Gamma = I_b\ddot{\alpha} + J^T m_s \ddot{D} - J^T m_s \vec{g} - \Gamma_{cm} \quad (21)$$

In this equation, $\Gamma = [\tau_1 \quad \tau_2 \quad \tau_3]^T$ is the driving torque of three joints. $\Gamma_{cm} = [\tau_{cm1} \quad \tau_{cm2} \quad \tau_{cm3}]^T$ is the gravity torque of three synthesized semi-discs. With $\ddot{D} = \dot{J}\dot{\alpha} + J\ddot{\alpha}$ it can also be described as:

$$\Gamma = (I_b + J^T J m_s)\ddot{\alpha} + J^T \dot{J} m_s \dot{\alpha} - J^T m_s \vec{g} - \Gamma_{cm} \quad (22)$$

Compare equation (1) and (21) we have:

$$M(\alpha) = I_b + J^T J m_s \quad (23)$$

$$C(\alpha, \dot{\alpha}) = J^T \dot{J} m_s \quad (24)$$

$$G(\alpha) = -J^T m_s \vec{g} - \Gamma_{cm} \quad (25)$$

3.3.3 Simulation

After inputting the relative equation and the physical parameters into MATLAB, the theoretical torque curve could be obtained. After importing the model into ADAMS and adjusting relative settings, we measure the driving torque and collect the data in Postprocessor, we name it as the simulation data.

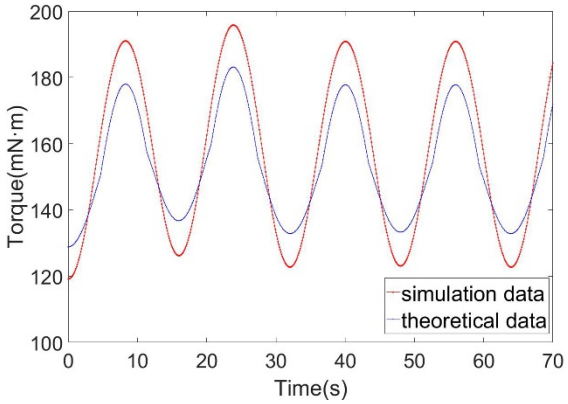

Figure 6: Simulation and theoretical torque of joint 1.

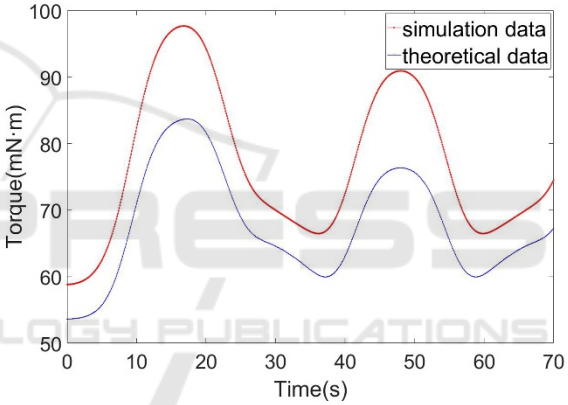

Figure 7: Simulation and theoretical torque of joint 2.

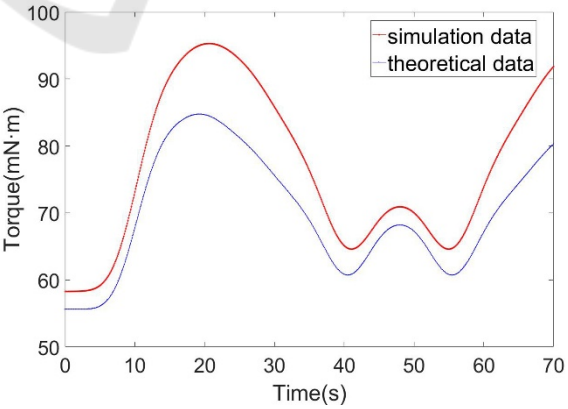

Figure 8: Simulation and theoretical torque of joint 3.

Although the theoretical data and the simulated data show the same trend, the difference still exists. The errors between the theoretical data and the

simulated data of the joints are shown in figure, the standard deviation of these three pairs of curve are $9.768mN \cdot m$, $9.854mN \cdot m$ and $7.44mN \cdot m$.

4 GRAVITY-COMPENSATION BASED ON BP NEURAL NETWORK

The errors mentioned above mainly come from two parts: the simplification of the model and the ignorance of the friction. In order to improve the result of gravity compensation, BP neural network is used to compensate the errors.

BP neural network includes input layer, output layer and hidden layers (Chu J, 2013). The connection between different layers relies on the nodes, the connection weights are different between different node units, they reflect the strength between layers and nodes is different (Li J, 2012). BP neural network uses Widrow-Hoff learning algorithm and non-linear transfer function. During the transfer process, the information is transmitted in the positive direction while the error is transmitted backwards. The information enters the network through the input layer, then it goes through the hidden layer and the output layer (Ma C, 2016). During the whole process, the output of the previous layer is the input of the next layer. If the final output doesn't meet the expectation, then transmit the error backwards and adjust the connection weights until the output meets the need. The BP neural network used in this paper can be described as:

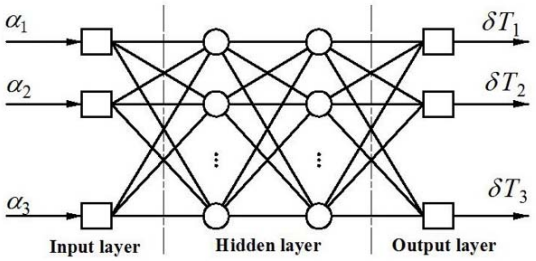

Figure 9: The structure of BP neural network.

The equation (22) can be changed as:

$$\Gamma_{BP} = \Gamma + \delta T \tag{26}$$

In this equation, Γ_{BP} is the driving torque, δT is the output of the neural network, which is also the compensated value of gravity compensation value.

Then we design the neural network for δT, the BP neural network used in this paper contains 4 layers, 2 hidden layers, 1 input layer and 1 output layer. Set the activation function of the output layer as the linear Purelin function and then set the activation function of the hidden layers as non-linear Tan-Sigmoid.

In this paper, we select the trainlm function as the training method, it is based on Levenberg-Marquardt algorithm. It is a kind of non-linear optimization method between Newton's method and gradient descent method, it can not only speed up the training speed, but also reduce the possibility of falling into the local minimum value. The design process is as follows:

Firstly, we determine the input vector and the expected response. Set the turning angle of the semi-discs' active joints $\alpha = [\alpha_1 \quad \alpha_2 \quad \alpha_3]^T$ as input, then set the errors between the driving torque and theoretical torque $\delta T = [\delta T_1 \quad \delta T_2 \quad \delta T_3]^T$ as the expected response, so the input and output layer both have 3 node units.

Secondly, we determine the node number on the hidden layers. We collected 28800 sets of sample data and all of them are in the workspace of the haptic device, it is shown in Figure 10. In the figure, green points represent the workspace, while the red ones represent the collected training data. In the training process, the performance detection algorithm uses the mean square error and it reaches its minimum value 1.5867×10^{-3} when the node number of the hidden layers are 13 and 15. After the training, save the neural network as a mat file.

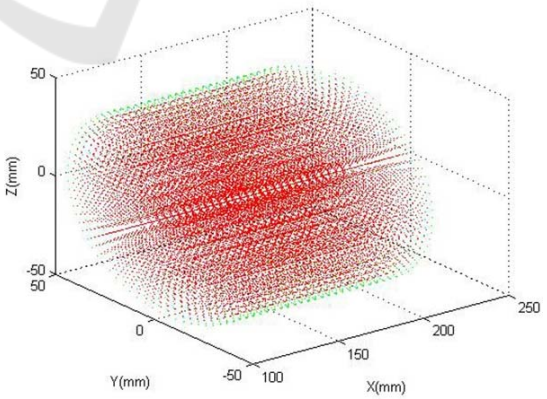

Figure 10: The workspace of the haptic device.

Thirdly, we test the performance of BP neural network. Collect 1024 sets of test data (all of the data is in the workspace of the haptic device) in ADAMS, and then calculate the error with the BP neural

network in MATLAB. After adding the error to equation (26), we can compare the simulation data collected by ADAMS and the compensated data calculated by MATLAB:

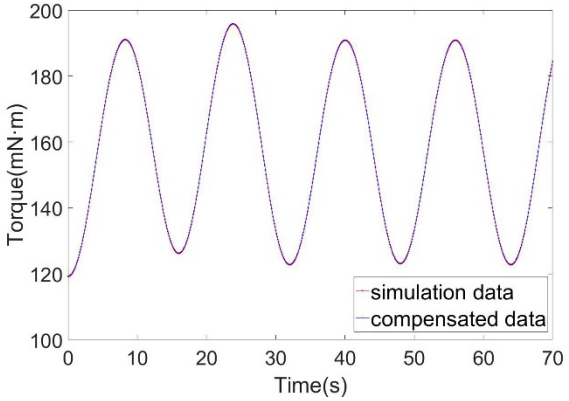

Figure 11: Simulation and compensated torque of joint 1.

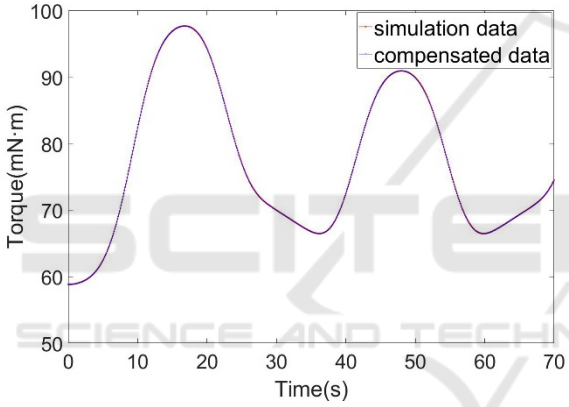

Figure 12: Simulation and compensated torque of joint 2.

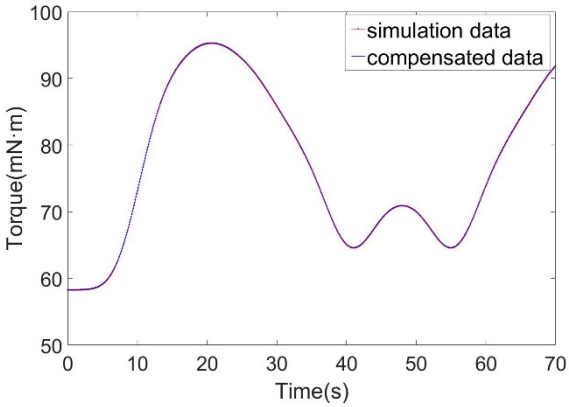

Figure 13: Simulation and compensated torque of joint 3.

From figures showed above, we can see that the curve of the simulation data and the curve of the compensated data almost coincide, the standard deviation of three pairs of curve reduces to $0.053mN \cdot m$, $0.0498mN \cdot m$ and $0.0302mN \cdot m$.

5 CONCLUSIONS

The research of the gravity compensation algorithm and its error compensation method of the haptic device had been conducted. When we analysed the system, we simplified the serial part as a whole and added its mass to the moving platform which was part of the parallel mechanism. Then we carried the dynamic modelling with the principle of virtual work and thereby fulfilling the goal of gravity compensation. After that we compared the curve of the simulation data and the curve of the compensated data and found the errors between them. In order to eliminate the errors, we designed a set of BP neural network. Under the help of neural network, the errors had been reduced greatly and this also proves the effectiveness of the BP neural network on the error elimination of gravity compensation.

REFERENCES

Codourey, A. 1998. Dynamic Modeling of Parallel Robots for Computed-Torque Control Implementation. *The International Journal of Robotics Research*, 17(12), pp.1325-1336.

Okamura, A., Verner, L., Reiley, C. and Mahvash, M. 2010. Haptics for Robot-Assisted Minimally Invasive Surgery. *Springer Tracts in Advanced Robotics*, pp.361-372.

Wang, J. and Gosselin, C. 1998. A new approach for the dynamic analysis of parallel manipulators. *Multibody System Dynamics*, 2(3), pp.317-334.

Zhang, L., Wang, S., Li, J. and Li, J. 2013. Design of a Master Manipulator with Dynamical Simplification for Master-Slave Robot. *Applied Mechanics and Materials*, 418, pp.3-9.

You, W., Kong, M., Du, Z. and Sun, L. 2008. High efficient inverse dynamic calculation approach for a haptic device with pantograph parallel platform. *Multibody System Dynamics*, 21(3), pp.233-247.

Wu, B., Han, S., Xiao, J., Hu, X. and Fan, J. 2016. Error compensation based on BP neural network for airborne laser ranging. *Optik - International Journal for Light and Electron Optics*, 127(8), pp.4083-4088.

Chu, J., Li, H. and Chen, X. 2013. Research on Improved BP Learning Algorithm of BP Neural Network. *Advanced Materials Research*, 765-767, pp.1644-1647.

Li, J., Cheng, J., Shi, J. and Huang, F. 2012. Brief Introduction of Back Propagation (BP) Neural Network Algorithm and Its Improvement. *Advances in Intelligent and Soft Computing*, pp.553-558.

Ma, C., Zhao, L., Mei, X., Shi, H. and Yang, J. (2016). Thermal error compensation of high-speed spindle system based on a modified BP neural network. *The International Journal of Advanced Manufacturing Technology*, 89(9-12), pp.3071-3085.